Original article

Energy storage in carbonate and basalt reservoirs: Investigating secondary imbibition in H_2 and CO_2 systems

Mirhasan Hosseini[1][ORCID]*, Muhammad Ali[1], Jalal Fahimpour[2], Alireza Keshavarz[1], Stefan Iglauer[1]

[1]*Petroleum Engineering Discipline, School of Engineering, Edith Cowan University, 270 Joondalup Dr, Joondalup, WA 6027, Australia*
[2]*Department of Petroleum Engineering, Amirkabir University of Technology, Tehran 15614, Iran*

Abstract:
Gas injection into geological storage sites displaces existing water in rock pore spaces, triggering lateral secondary imbibition. This phenomenon involves the migration of water from areas with higher water saturation to replenish the displaced water. The lateral distance over which this imbibition occurs is critical for understanding injection/withdrawal flow rates and trapped-gas saturation during hydrogen and carbon dioxide geological storage. This study investigates secondary imbibition dynamics in hydrogen and carbon dioxide systems for calcite (representing carbonates) and basalt, considering pressure and temperature effects. Utilizing the modified Lucas-Washburn equation, the results reveal that lateral distance and secondary imbibition rates of water for all gas and rock systems decline with pressure. Additionally, the lateral distance and secondary imbibition rate of water for the hydrogen system at carbonates and basalts, and the carbon dioxide system at carbonates, increase with temperature. However, the lateral distance and secondary imbibition rate of water for the carbon dioxide system at basalts decrease with temperature. This research provides crucial fundamental data with significant implications for underground hydrogen storage and carbon dioxide geological storage. The findings contribute to the understanding of lateral imbibition in carbonate and basaltic rocks, offering valuable insights for enhancing gas retention within pore spaces, thereby influencing residual trapping.

1. Introduction

In recent years, large-scale gas storage has been increasingly important for energy transition or "Net-Zero" targets (Tarkowski, 2019; Hassanpouryouzband et al., 2020b; Zivar et al., 2021; Xu et al., 2022). For example, the reduction of dependency on fossil fuels (e.g., oil and coal) in power generation requires the production and storage of more renewable resources (e.g., hydrogen production and storage) (Helm, 2016; Michaelides, 2017; Hassanpouryouzband et al., 2018; Palmer, 2019). In addition, the permanent removal of carbon dioxide (CO_2) from the atmosphere requires carbon capture and storage technology (Lackner et al., 2003; Hassanpouryouzband et al., 2019; Pentland et al., 2021; Isfehani et al., 2023; Zhang et al., 2023).

Geological formations, including reservoir rocks or salt caverns made through the process of dissolving salt in deep salt beds by circulating water injected through a well, provide large-scale gas storage capacities (Pfeiffer and Bauer, 2015; Hemme and Berk, 2018; Zeng et al., 2022). However, geological gas storage is implemented for different purposes. For example, hydrogen gas as a clean fuel is temporarily trapped in geological formations (a process known as underground hydrogen storage (UHS)) and withdrawn again for power generation at peak demand times (Hassanpouryouzband et al., 2020a; Muhammed et al., 2022). Whereas, CO_2 geological storage (CGS) is a long-term solution for permanent locking away of gas and enhanced hydrocarbon recovery (Blunt et al., 1993; Metz et al., 2005; Boot-Handford et al., 2014; Ettehadtavakkol et al., 2014). CO_2 may also be used as a cushion gas for hydrogen recovery at peak demand times by retaining adequate reservoir pressure to keep the hydrogen withdrawal stable (Isfehani et al., 2023).

Fluid dynamics such as drainage and imbibition in porous medium play important roles in simulating and developing models for predicting UHS and CGS performances (Cai and Yu, 2011; Hashemi et al., 2021; Zivar et al., 2021). In this regard, spontaneous imbibition (SI) is a process in which a wetting phase (e.g., formation brine) displaces a fraction of the non-wetting phase (e.g., injected gas) via capillary suction in a porous medium (Mason and Morrow, 2013; Iglauer et al., 2015; Yang et al., 2018; Gao et al., 2019). For example, for a water-wet reservoir rock where hydrogen has been stored, SI is defined as the re-imbibition of brine (displacing the mobile-gas phase) in the rock when hydrogen is withdrawn (Cai et al., 2014; Zivar et al., 2021). Another example is for CGS process where the CO_2 plume migrates from the injection point and then water re-imbibes the pore space of the formation (Li et al., 2012; Herring and Andersson, 2016; Zhang et al., 2022). This re-imbibition process is continued until a trapped-gas saturation is achieved, which is known as residual gas trapping (Bennion and Bachu, 2008; Iglauer et al., 2015; Cai et al., 2022). The gas mobilities during drainage and imbibition processes are different, reflecting the effect of hysteresis on capillary pressure curves (Plug et al., 2007). This hysteresis is specifically important for hydrogen geological storage where gas injection/withdrawal operation is cyclic (Zivar et al., 2021). The increase in the number of hydrogen injection/withdrawal cycles (capillary hysteresis) leads to an increase in the trapped-hydrogen (H_2) saturation and consequently, a reduction in the efficiency of hydrogen recovery (Carden and Paterson, 1979; Hashemi et al., 2021), which is not favorable for short-term gas geo-storage purposes. However, an increase in the trapped-CO_2 saturation in a rock indicates more residual storage capacity for CO_2 which is favorable for successful sequestration and long-term containment security of CO_2 (Tokunaga et al., 2013; Iglauer et al., 2015).

The literature data for determining the SI dynamics at geo-storage conditions are scarce. So far, Pan et al. (2022) have used the modified Lucas-Washburn equation to compute the SI dynamics of brine in small capillary tubes of sandstone for methane (CH_4), H_2, and CO_2 systems under geo-storage conditions. They found that SI rates for H_2 and CH_4 increase with formation depth, however, this phenomenon is reversed for CO_2. They also showed that the SI rate decreases in the presence of organic matter and can be increased with silica nanofluid aging.

Thus, there is a clear paucity of data for SI dynamics for carbonate and basaltic rocks at geo-storage conditions. Calcites, representing carbonate reservoir rocks, are usually characterized by high porosity and permeability, providing favorable conditions for fluid migration and storage (Tonnet et al., 2011; Haldar, 2020). Basaltic rocks, prevalent in volcanic regions such as the mid-ocean ridges, exhibit distinct geological features, including a dense, fine-grained matrix with low to moderate porosity and permeability (Selley et al., 2005).

The present study seeks to address this gap by applying the modified Lucas-Washburn equation to investigate SI dynamics in H_2 and CO_2 systems for calcite and basalt under varying pressure and temperature conditions. The aim is to contribute fundamental data that will enhance the understanding of SI behaviors, crucial for optimizing gas storage projects in carbonate and basaltic rocks. In considering the research status, it is evident that while the general principles of imbibition and drainage are well-established, the specific dynamics in carbonate and basaltic rocks, especially under geo-storage conditions, warrant a more comprehensive exploration. The present study, focusing on these specific geological formations, aims to bridge this knowledge gap and offer insights that can inform future advancements in underground gas storage technologies. This work thus provides fundamental data for the successful fulfillment of the UHS and CGS in carbonate and basaltic rocks.

2. Methodology

By assuming a series of small parallel capillary tubes for the porous rock, the fluid velocity (v_i where i denotes the wetting (w) and non-wetting (nw) phases) in the rock is defined as the fluid displacement (L_i) in the small capillary tubes at a given time (t):

$$v_i = \frac{dL_i}{dt} \qquad (1)$$

The fluid flow through porous medium can be described by Darcy's law (Neuman, 1977):

$$v_i = -\frac{kk_{ri}}{\mu_i}(\nabla p_i - \rho_i g) \qquad (2)$$

where k is the rock permeability, k_{ri} is the relative permeability, μ_i is the fluid viscosity, ∇p_i is the pressure gradient, ρ_i is the fluid density, and g is the gravitational acceleration. By neglecting the gravity and gas/water counter-current flow and combining Eqs. (1)-(2), the following equation is obtained:

$$\frac{dL_i}{dt} = -\frac{kk_{ri}p_i}{\mu_i L_i} \qquad (3)$$

The capillary pressure is obtained by the Young-Laplace equation:

$$p_c = p_{nw} - p_w = \frac{2\gamma\cos\theta_a}{r} \qquad (4)$$

where γ is the gas-water interfacial tension, θ_a is the advancing water contact angle in a rock/gas/water system, and r is the mean pore throat radius. Behind the imbibition front, the parallel capillary tubes are assumed to be entirely saturated with water (e.g., $S_w = 100\%$ and $k_{rw} = 1$). Thus, the following equation is obtained by the combination of Eqs. (3)-(4):

$$\frac{dL_w}{dt} = \frac{2k\gamma\cos\theta_a}{r\mu_w L_w} \qquad (5)$$

Integrating Eq. (5) and assuming $L_w (t = 0) = 0$, the following equation is obtained:

$$L_w = \sqrt{4t\frac{k}{r}\frac{\gamma}{\mu_w}\cos\theta_a} \qquad (6)$$

Eq. (6) is the modified Lucas-Washburn equation which is used to determine the distance (L) for secondary imbibed formation brine in small capillary tubes of carbonate and basaltic rocks at a given time (t) (Lucas, 1918; Washburn, 1921;
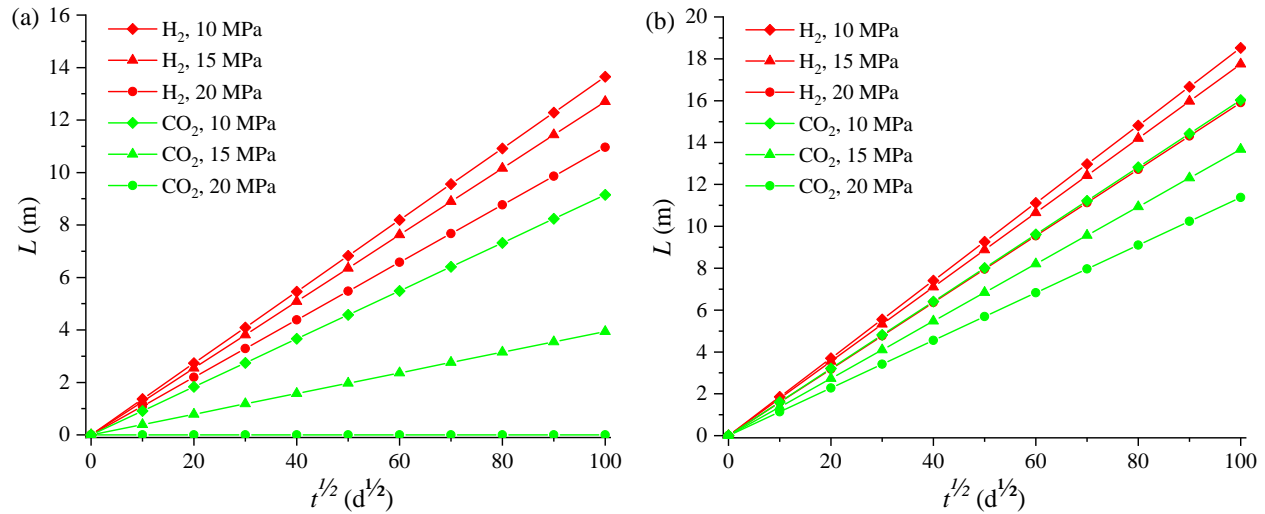
Fig. 1. Effect of pressure and temperature on water secondary imbibition in carbonates. (a) 323 K for H_2 and CO_2 systems, and (b) 353 K for H_2 and 343 K for CO_2. Readers are referred to Arif et al. (2017) and Hosseini et al. (2022c) for θ_a data, Li et al. (2012) and Hosseini et al. (2022b) for γ data, and Kestin et al. (1981) for μ data.

Pan et al., 2021). It is clear from Eq. (6) that there is an ideally linear relationship between L and $\sqrt{t}$. In addition to this, the parameters are categorized into three groups. The k and r reflect the rock properties, γ and μ reflect the fluid properties, and θ_a reflects the rock-fluid interaction or wettability (note: advancing contact angle is associated with the imbibition process, where the fluid infiltrates the porous medium, while receding contact angle is associated with the drainage process, where the fluid is expelled from the porous medium (Iglauer et al., 2015)). In is notable that the modified Lucas-Washburn equation is not valid for the intricate reservoir conditions as many relevant factors such as initial water saturation, irreducible gas saturation, gas viscosity, gas density, gas compressibility, mutual solubility of gas and water, pore size distribution, rock mineralogy, layer geometry have not been accounted in Eq. (6). Furthermore, the utilization of Eq. (6) is restricted when dealing with gas-wet carbonate or basaltic rocks, where θ is greater than 90° or the $\cos\theta$ is negative. Thus, the following discussion is obtained for the simplified reservoir conditions to analyze the variation of L with the relevant parameters in the equation.

3. Results

Subsurface formations have different pressure and temperature values (Djebbar and Donaldson, 2012; Hosseini et al., 2014; Hosseini, 2016), it is thus important to characterize L as a function of pressure and temperature. All the parameters given in Eq. (6) are affected by pressure and temperature. However, the assumed constant (homogeneous) rock properties for carbonate and basaltic rocks. For carbonate rock, $k = 10$ mD and $r = 10$ μm were assumed as it is a sedimentary rock, however, for basaltic rock, $k = 10$ nD and $r = 10$ nm were assumed as it is an igneous rock. Thus, the effect of other fluids, interface, and wetting characteristics of the rock/gas/water systems (taken from the literature (Kestin et

al., 1981; Li et al., 2012; Arif et al., 2017; Iglauer et al., 2020; Hosseini et al., 2022b, 2022c)) on the SI dynamics can be easily evaluated. Notably, clean carbonate and basalt samples (without aging in organic acids or other chemicals) were analyzed in this study.

3.1 Effect of pressure and temperature on water secondary imbibition in carbonates

For both H_2 and CO_2 systems in carbonates, L and SI rates decreased with pressure, Fig. 1 and Table 1. For instance, at 323 K after 10,000 days for the H_2 system, L and SI rates decreased from 13.65 to 10.96 m and 0.14 to 0.11 m·d$^{-0.5}$, respectively, when pressure increased from 10 to 20 MPa. In addition, at similar physio-thermal geological conditions and similar injection time for the CO_2 system, L and SI rates decreased from 9.15 to 0 m and 0.09 to 0 m·d$^{-0.5}$, respectively, implying that there is no SI dynamics when the rock becomes gas-wet (Iglauer et al., 2015). However, for both H_2 and CO_2 systems in carbonates, L and SI rates increased with temperature, Fig. 1 and Table 1. For instance, at 20 MPa after 10,000 days for the H_2 system, L and SI rates increased from 10.96 to 15.90 m and 0.16 to 0.19 m·d$^{-0.5}$, respectively, when the temperature increased from 323 to 353 K. In addition to this, at similar physio-thermal geological conditions and at similar injection time for CO_2 system, L and SI rates increased from 0 to 11 m and 0 to 0.11 m·d$^{-0.5}$, respectively.

3.2 Effect of pressure and temperature on water secondary imbibition in basaltic rocks

Analogous to the carbonates, both H_2 and CO_2 systems in basalts showed reductions in L and SI rates with pressure, Fig. 2 and Table 2. However, the variations in L and SI rates with pressure for both H_2 and CO_2 systems in the basalts are very low compared to the carbonates. For instance, at 308 K after 10,000 days for the H_2 system, L and SI rates

Table 1. Water secondary imbibition rate in carbonates for H_2 and CO_2 systems.

System	T (K)	p (MPa)	γ (mN/m)	$\cos\theta_a$	μ (mPa·s)	SI rate (m·d$^{-0.5}$)
		10	67.98	0.44	0.5489	0.1365
	323	15	67.38	0.38	0.5498	0.1270
		20	66.77	0.29	0.5506	0.1096
H_2		10	61.90	0.57	0.3576	0.1852
	353	15	61.43	0.53	0.3588	0.1774
		20	60.96	0.43	0.3600	0.1590
		10	35.5	0.37	0.5489	0.0915
	323	15	29	0.09	0.5498	0.0394
		20	26	0	0.5506	0
CO_2		10	43	0.70	0.407	0.1592
	343	15	34.5	0.64	0.4082	0.1367
		20	27	0.57	0.4094	0.1138

Note: The data for μ, γ, and θ_a are taken from Kestin et al. (1981); Li et al. (2012); Arif et al. (2017); Hosseini et al. (2022b, 2022c).
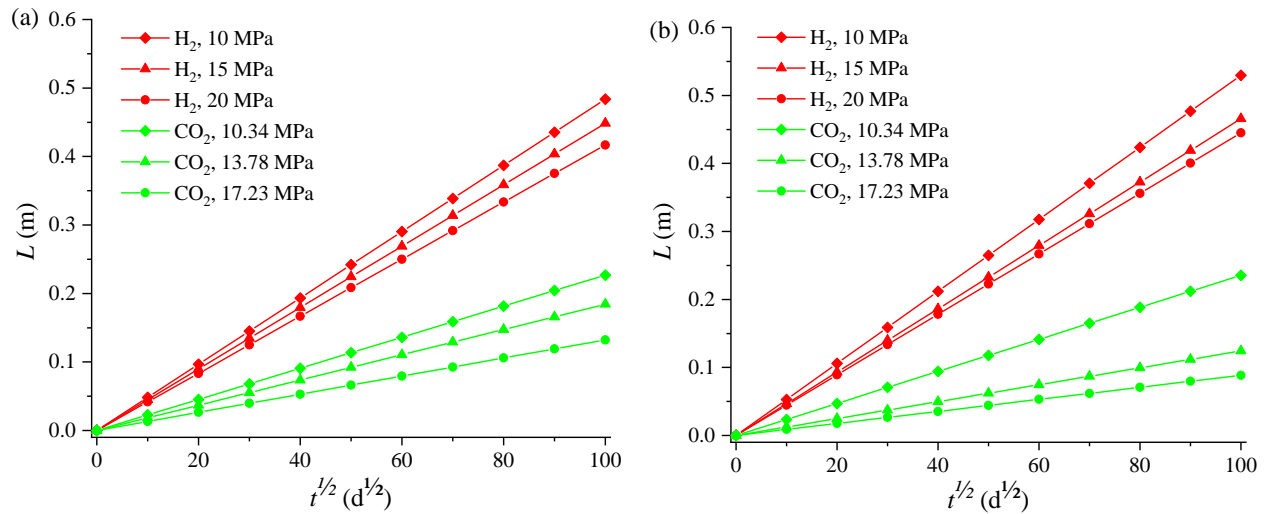

Fig. 2. Effect of pressure and temperature on water secondary imbibition in basalts. (a) 308 K for H_2 and CO_2 systems, and (b) 343 K for H_2 and 333 K for CO_2. Readers are referred to Iglauer et al. (2020) and Hosseini et al. (2022a) for θ_a data, Li et al. (2012) and Hosseini et al. (2022b) for γ data, and Kestin et al. (1981) for μ data.

decreased from 0.48 to 0.42 m and 0.0048 to 0.0042 m·d$^{-0.5}$, respectively, when pressure increased from 10 to 20 MPa. In addition, at similar physio-thermal geological conditions and similar injection times for the CO_2 system, L and SI rates decreased from 0.23 to 0.13 m and 0.0023 to 0.0013 m·d$^{-0.5}$, respectively. Moreover, for the H_2 system in basalts, L and SI rates slightly increased with temperature, Fig. 2 and Table 2. For instance, at 20 MPa after 10,000 days for the H_2 system, L and SI rates increased slightly from 0.42 to 0.45 m and 0.0042 to 0.0045 m·d$^{-0.5}$, respectively, when the temperature increased from 308 to 343 K. However, for the CO_2 system in basalts, L and SI rates generally increased slightly with temperature, Fig. 2 and Table 2. For instance, at 17.23 MPa

after 10,000 days for the CO_2 system, L and SI rates decreased from 4.18 to 2.8 m and 0.04 to 0.03 m·d$^{-0.5}$, respectively, when the temperature increased from 308 to 333 K.

4. Discussion

Understanding the behavior of SI dynamics in gas storage scenarios is crucial for optimizing UHS and CGS projects. The parameters μ, γ, and θ_a play a pivotal role in influencing SI rates and L in carbonate and basaltic rocks. The impact of pressure and temperature on these parameters is a key focus of the analysis.

Table 2. Water secondary imbibition rate in basalts for H_2 and CO_2 systems.

System	T (K)	p (MPa)	γ (mN/m)	$\cos\theta_a$	μ (mPa·s)	SI rate (m·d$^{-0.5}$)
		10	72.33	0.67	0.7194	0.0048
	308	15	71.61	0.58	0.7195	0.0045
		20	70.88	0.51	0.7197	0.0042
H_2		10	65.46	0.50	0.407	0.0053
	343	15	64.89	0.39	0.4082	0.0047
		20	64.32	0.36	0.4094	0.0045
		10	31.18	0.34	0.7194	0.0023
	308	15	29.55	0.24	0.7195	0.0018
		20	28.71	0.13	0.7197	0.0013
CO_2		10	37.7	0.20	0.47795	0.0024
	333	15	34.4	0.06	0.479	0.0012
		20	32.95	0.03	0.48	0.0009

Note: The data for μ, γ, and θ_a are taken from Kestin et al. (1981); Li et al. (2012); Iglauer et al. (2020); Hosseini et al. (2022a, 2022b).

4.1 Pressure-dependent analysis

Analyzing the pressure-dependent trends, distinct behaviors were observed in carbonate rocks for both H_2 and CO_2 systems.

4.1.1 H_2 system in carbonate rock

In the H_2 system, increasing pressure results in a rise in θ_a and a decrease in γ, while μ shows a slight increase. For example, when pressure increased from 10 to 20 MPa at 323 K, θ_a in carbonate rock increased from 64.2° to 73.35° (decrease in $\cos\theta_a$ due to the increased intermolecular forces between gas and rock with pressure (Arif et al., 2017; Hosseini et al., 2022c)) and γ decreased from 67.98 to 66.77 mN/m (due to the increased intermolecular forces between gas and liquid with pressure (Hosseini et al., 2022b)), while μ slightly increased from 0.5489 to 0.5506 mPa·s.

4.1.2 CO_2 system in carbonate rock

The CO_2 system in carbonate rock exhibits contrasting trends in θ_a, γ, and μ with pressure. For example, when pressure increased from 10 to 20 MPa at 323 K, θ_a in carbonate rock increased from 68° to 90° (decrease in $\cos\theta_a$) and γ decreased from 35.5 to 26 mN/m, but μ slightly increased from 0.5489 to 0.5506 mPa·s. Thus, for both H_2 and CO_2 systems in carbonate rock, all three parameters (θ_a, γ, and μ) were effective in the trend/rate of L with pressure, although the effects of θ_a and γ are more tangible than μ on this trend/rate. More values of L for the H_2 system compared to the CO_2 system in carbonate rock are attributed to the high γ and $\cos\theta_a$ values for the H_2 system. However, more decrease in SI rate with pressure for the CO_2 system compared to the H_2 system in carbonate rock is attributed to the more decrease in γ and $\cos\theta_a$ for the CO_2 system.

4.1.3 H_2 and CO_2 system in basaltic rock

The reductions in L and SI rates with pressure for basaltic rock are extremely lower than in carbonate rock. This is attributed to the low rock properties (k and r) for the basalts compared to the carbonates. However, this very smooth change in trend/rate of L with pressure and temperature in basalts can also be interpreted by the change in θ_a, γ, and μ with pressure and temperature. The effects of pressure on θ_a, γ, and μ in the basaltic rocks are similar to the carbonates. For the H_2 system, when pressure increased from 10 to 20 MPa at 308 K, θ_a in basaltic rock increased from 47.68° to 59.31° (decrease in $\cos\theta_a$ (Hosseini et al., 2022a)) and γ decreased from 72.33 to 70.88 mN/m, while μ slightly increased from 0.7194 to 0.7197 mPa·s. Similarly, for the CO_2 system at the same temperature when pressure increased from 10.34 to 17.23 MPa, θ_a in basaltic rock increased from 69.88° to 82.70° (decrease in $\cos\theta_a$) and γ decreased from 31.18 to 28.71 mN/m, but μ slightly increased from 0.7194 to 0.7196 mPa·s. Thus, for both H_2 and CO_2 systems in basaltic rock, all three parameters (θ_a, γ, and μ) were effective in the trend/rate of L with pressure, although the effects of θ_a and γ are more tangible than μ on this trend/rate. Analogous to the carbonates, the H_2 system in basalts has more values of L compared to the CO_2 system due to the higher values of γ and $\cos\theta_a$. In addition to this, as γ and $\cos\theta_a$ decrease more for the CO_2 system, more decrease in SI rate with pressure was observed for the CO_2 system compared to the H_2 system in basaltic rocks.

4.2 Temperature-dependent analysis

Shifting the attention to temperature-dependent trends, nuanced behaviors were observed in carbonate rocks.

Table 3. Effectiveness of the parameters in the trend of distance.

Trend of distance	θ_a	γ	μ
With pressure for H_2 in carbonates	√	√	√
With pressure for CO_2 in carbonates	√	√	√
With pressure for H_2 in basalts	√	√	√
With pressure for CO_2 in basalts	√	√	√
With temperature for H_2 in carbonates	√	/	√
With temperature for CO_2 in carbonates	√	√	√
With temperature for H_2 in basalts	/	/	√
With temperature for CO_2 in basalts	/	√	√

4.2.1 H_2 system in carbonate rock

For the H_2 system, when temperature increased from 323 to 353 K at 20 MPa, θ_a in carbonate rock decreased from 73.55° to 64.4° (increase in $\cos\theta_a$ due to the decreased molecular interactions between gas and rock surface with temperature (Hosseini et al., 2022c)) and γ decreased from 66.77 to 60.96 mN/m (due to the decreased density difference between hydrogen and water with temperature (Hosseini et al., 2022b)), while μ decreased from 0.5506 to 0.36 mPa·s (due to the increased water molecular momentum and thermal motion with temperature (Bird, 2002)). Thus, for the H_2 system in carbonates, two parameters (θ_a and μ) were more effective in the trend/rate of L with temperature.

4.2.2 CO_2 system in carbonate rock

The CO_2 system in carbonate rocks demonstrates different trends in θ_a, γ, and μ with temperature. For example, for the CO_2 system at the same pressure when temperature increased from 323 to 343 K, θ_a in carbonate rock decreased from 90° to 55.4° (increase in $\cos\theta_a$) and γ slightly increased from 26 to 27 mN/m (due to the increased density difference between CO_2 and water with temperature (Hosseini et al., 2022b)), while μ decreased from 0.5506 to 0.4094 mPa·s. Thus, for the CO_2 system in carbonates, all three parameters (θ_a, γ, and μ) were effective in the trend/rate of L with temperature. More increase in SI rate with temperature for CO_2 system compared to H_2 system in carbonate rock is attributed to the more increase in $\cos\theta_a$ for CO_2 system and different behaviors of γ with temperature for H_2 and CO_2 systems.

4.2.3 H_2 and CO_2 system in basaltic rock

The variations in L and SI rates with temperature for both H_2 and CO_2 systems in the basalts have behaved similarly and remained very low compared to the carbonates. For an increase in temperature from 308 to 234 K at 20 MPa for H_2 system, θ_a in basaltic rock increased from 59.31° to 68.61° (decrease in $\cos\theta_a$), γ decreased from 70.88 to 64.32 mN/m, and μ decreased from 0.7197 to 0.4094 mPa·s. Thus, for the H_2 system in basalts, μ was the most effective parameter in the trend/rate of L with temperature. However, for CO_2 system in basaltic rock, when temperature increased from 308 to 333 K at 17.23 MPa, θ_a increased from 82.70° to 88.11° (decrease in $\cos\theta_a$), γ increased from 28.71 to 32.95 mN/m, and μ decreased from 0.7180 to 0.48 mPa·s. Thus, for the CO_2 system in basalts, γ and μ were the most effective parameters in the trend/rate of L with temperature.

4.3 Summary of findings

Generally, the effect of temperature on the changes of SI rate in carbonates is considerably more than in basalts, which particularly refers to the difference in the rock properties (k and r) and the change of $\cos\theta_a$ with temperature for both rocks. Table 3 specifies the effectiveness of the parameters (mentioned in Eq. (6)) in the trend of L with pressure and temperature for various systems examined in this study. The analysis reveals that all three parameters play a crucial role in the trend of L with pressure across all systems studied. Except for CO_2 in carbonates, the trend of L with temperature is primarily influenced by one or two parameters in all the other systems.

4.4 Implications for gas storage

Expanding the analysis to the implications for gas storage capacity, the characterization of secondary imbibition in carbonates and basalts becomes pivotal. Assessing the gas storage potential, particularly the CO_2 residual trapping capacity, is essential for informed decision-making in storage projects (Iglauer et al., 2015; Al-Khdheeawi et al., 2017a, 2017b). When more lateral secondary imbibition of water occurs in a geo-storage site, such as in cyclic gas storage operations, it results in increased gas trapping in the pores (Niu et al., 2015; Herring and Andersson, 2016; Edlmann et al., 2019). This phenomenon is favorable for long-term CO_2 storage, as more trapped CO_2 translates to enhanced storage capacity. However, the same may not hold true for short-term H_2 storage, where more trapped H_2 could lead to less H_2 recovery (Carden and Paterson, 1979; Tokunaga et al., 2013; Hashemi et al., 2021). These contrasting dynamics underscore the importance of tailoring gas storage strategies based on the specific characteristics of the rock formations. Moreover, the pressure and temperature dependence of secondary imbibition dynamics opens avenues for strategic planning in different gas geo-storage projects. For instance, high-pressure carbonate formations may lead to low residual storage for both H_2 and CO_2, favoring UHS but proving unfavorable for CGS. On the other hand, hot carbonate formations may result in high residual storage for both gases, making them favorable for CGS but less suitable for UHS. In contrast, basaltic formations, characterized by low L and SI rates, are generally favorable for UHS but less so for CGS due to their very low permeability and pore throat size.

4.5 Limitations and future directions

In this study, constant rock properties (permeability and pore size) were assumed for both carbonate and basaltic rocks (uniform and homogeneous pore structures). However, these two parameters can be different in the rocks (heterogeneous porous medium), which affects the SI dynamics due to devi-

ations from the idealized Lucas-Washburn model (Bakhshian et al., 2020; Qin et al., 2022). This means that the SI rate and the spreading of the wetting fluid may not follow the traditional square-root-of-time relationship predicted by the Lucas-Washburn model. In other word, heterogeneity can lead to fingering or channeling effects, where the wetting fluid preferentially flows through certain pathways while bypassing other regions. This non-uniform fluid distribution further deviates from the assumptions of the Washburn model. Moreover, the extent and type of organic matter in the rocks, along with the brine salinity, are additional factors that influence the parameters being considered (θ_a, γ, and μ) (Ali et al., 2022; Hosseini et al., 2022a, 2022c), and thus the SI dynamics. Therefore, the effects of pore-scale heterogeneity, pore connectivity, brine salinity and organic matter properties are other aspects for future research that need to be carefully examined. Although this study focuses on separately analyzing the SI of H_2 and CO_2 systems for pure gas storage scenarios, the same analysis can be conducted when the gases are mixed, such as when CO_2 is used as a cushion gas for H_2. However, due to the lack of sufficient data for such calculations, it is recommended as a topic for future research. It is important to note that while this study provides valuable insights into SI dynamics in H_2 and CO_2 systems for calcite and basalt, certain limitations are acknowledged. Notably, the effects of gas adsorption and desorption on SI and L were not explicitly considered in the analysis. Future investigations could explore these aspects to provide a more comprehensive understanding of gas retention mechanisms during geological storage.

5. Conclusions

The lateral secondary imbibition of water in a gas geo-storage formation is a key parameter affecting the injection/withdrawal flow rates and the trapped-gas saturation (Al-Khdheeawi et al., 2017a, 2017b; Cai et al., 2020; Pan et al., 2022). Nevertheless, there is a shortage of literature information regarding the SI dynamics in carbonate and basaltic rocks under conditions relevant to geological storage. Therefore, in this study, the modified Lucas-Washburn equation was applied to calculate the SI dynamics in H_2 and CO_2 systems for calcite (as a proxy for carbonates) and basalt as a function of pressure and temperature. The results showed that in the case of gas residual trapping, high-pressure carbonate and basaltic formations are favorable for H_2, but not favorable for CO_2 (specifically in carbonates). Moreover, hot carbonate formations lead to more trapped H_2 (unfavorable, less H_2 recovery), but more trapped CO_2 (favorable, more CO_2 storage capacity). In general, the basaltic formations are favorable for UHS but unfavorable for CGS (due to their very low L and SI rates). It is concluded that depending on the gas and rock type, geo-storage conditions (such as pressure and temperature) can affect the SI dynamics, which is crucial for optimization of gas geo-storage capacity (e.g., residual trapping capacity) with containment security during UHS and CGS projects.

Conflict of interest

The authors declare no competing interest.

References

Ali, M., Yekeen, N., Ali, M., et al. Effects of various solvents on adsorption of organics for porous and nonporous quartz/CO_2/brine systems: Implications for CO_2 geo-storage. Energy and Fuels, 2022, 36(18): 11089-11099.

Al-Khdheeawi, E. A., Vialle, S., Barifcani, A., et al. Impact of reservoir wettability and heterogeneity on CO_2-plume migration and trapping capacity. International Journal of Greenhouse Gas Control, 2017a, 58: 142-158.

Al-Khdheeawi, E. A., Vialle, S., Barifcani, A., et al. Influence of injection well configuration and rock wettability on CO_2 plume behaviour and CO_2 trapping capacity in heterogeneous reservoirs. Journal of Natural Gas Science and Engineering, 2017b, 43: 190-206.

Arif, M., Lebedev, M., Barifcani, A., et al. CO_2 storage in carbonates: Wettability of calcite. International Journal of Greenhouse Gas Control, 2017, 62: 113-121.

Bakhshian, S., Murakami, M., Hosseini, S. A., et al. Scaling of imbibition front dynamics in heterogeneous porous media. Geophysical Research Letters, 2020, 47(14): e2020GL087914.

Bennion, D. B., Bachu, S. Drainage and imbibition relative permeability relationships for supercritical CO_2/brine and H_2S/brine systems in intergranular sandstone, carbonate, shale, and anhydrite rocks. SPE Reservoir Evaluation & Engineering, 2008, 11(3): 487-496.

Bird, R. B. Transport phenomena. Applied Mechanics Reviews, 2002, 55(1): R1-R4.

Blunt, M., Fayers, F. J., Orr Jr, F. M. Carbon dioxide in enhanced oil recovery. Energy Conversion and Management, 1993, 34(9-11): 1197-1204.

Boot-Handford, M. E., Abanades, J. C., Anthony, E. J., et al. Carbon capture and storage update. Energy & Environmental Science, 2014, 7(1): 130-189.

Cai, J., Chen, Y., Liu, Y., et al. Capillary imbibition and flow of wetting liquid in irregular capillaries: A 100-year review. Advances in Colloid and Interface Science, 2022, 304: 102654.

Cai, J., Li, C., Song, K., et al. The influence of salinity and mineral components on spontaneous imbibition in tight sandstone. Fuel, 2020, 269: 117087.

Cai, J., Perfect, E., Cheng, C. L., et al. Generalized modeling of spontaneous imbibition based on hagen-poiseuille flow in tortuous capillaries with variably shaped apertures. Langmuir, 2014, 30(18): 5142-5151.

Cai, J., Yu, B. A discussion of the effect of tortuosity on the capillary imbibition in porous media. Transport in Porous Media, 2011, 89(2): 251-263.

Carden, P., Paterson, L. Physical, chemical and energy aspects of underground hydrogen storage. International Journal of Hydrogen Energy, 1979, 4(6): 559-569.

Djebbar, T., Donaldson, E. C. Theory and Practice of Measuring Reservoir Rock and Fluid Transport Properties. Amsterdam, The Kingdom of the Netherlands, Gulf Professional Publishing, 2012.

Edlmann, K., Hinchliffe, S., Heinemann, N., et al. Cyclic CO_2-H_2O injection and residual trapping: Implications for CO_2 injection efficiency and storage security. International Journal of Greenhouse Gas Control, 2019, 80: 1-9.

Ettehadtavakkol, A., Lake, L. W., Bryant, S. L. CO_2-eor and storage design optimization. International Journal of Greenhouse Gas Control, 2014, 25: 79-92.

Gao, Z., Fan, Y., Hu, Q., et al. A review of shale wettability characterization using spontaneous imbibition experiments. Marine and Petroleum Geology, 2019, 109: 330-338.

Haldar, S. K. Introduction to Mineralogy and Petrology. Amsterdam, The Kingdom of the Netherlands, Elsevier, 2020.

Hashemi, L., Blunt, M., Hajibeygi, H. Pore-scale modelling and sensitivity analyses of hydrogen-brine multiphase flow in geological porous media. Scientific Reports, 2021, 11(1): 8348.

Hassanpouryouzband, A., Joonaki, E., Edlmann, K., et al. Thermodynamic and transport properties of hydrogen containing streams. Scientific Data, 2020a, 7(1): 222.

Hassanpouryouzband, A., Joonaki, E., Farahani, M. V., et al. Gas hydrates in sustainable chemistry. Chemical Society Reviews, 2020b, 49(15): 5225-5309.

Hassanpouryouzband, A., Yang, J., Okwananke, A., et al. An experimental investigation on the kinetics of integrated methane recovery and CO_2 sequestration by injection of flue gas into permafrost methane hydrate reservoirs. Scientific Reports, 2019, 9(1): 16206.

Hassanpouryouzband, A., Yang, J., Tohidi, B., et al. CO_2 capture by injection of flue gas or CO_2-N_2 mixtures into hydrate reservoirs: Dependence of CO_2 capture efficiency on gas hydrate reservoir conditions. Environmental Science Technology, 2018, 52(7): 4324-4330.

Helm, D. The future of fossil fuels-is it the end? Oxford Review of Economic Policy, 2016, 32(2): 191-205.

Hemme, C., Berk, W. V. Hydrogeochemical modeling to identify potential risks of underground hydrogen storage in depleted gas fields. Applied Sciences, 2018, 8(11): 2282.

Herring, A. L., Andersson, L., Wildenschild, D. Enhancing residual trapping of supercritical CO_2 via cyclic injections. Geophysical Research Letters, 2016, 43(18): 9677-9685.

Hosseini, M. Estimation of mean pore-size using formation evaluation and stoneley slowness. Journal of Natural Gas Science and Engineering, 2016, 33: 898-907.

Hosseini, M., Ali, M., Fahimpour, J., et al. Basalt-H_2-brine wettability at geo-storage conditions: Implication for hydrogen storage in basaltic formations. Journal of Energy Storage, 2022a, 52: 104745.

Hosseini, M., Fahimpour, J., Ali, M., et al. H_2-brine interfacial tension as a function of salinity, temperature, and pressure; implications for hydrogen geo-storage. Journal of Petroleum Science and Engineering, 2022b, 213: 110441.

Hosseini, M., Fahimpour, J., Ali, M., et al. Hydrogen wettability of carbonate formations: Implications for hydrogen geo-storage. Journal of Colloid and Interface Science, 2022c, 614: 256-266.

Hosseini, M., Javaherian, A., Movahed, B. Determination of permeability index using stoneley slowness analysis, nmr models, and formation evaluations: A case study from a gas reservoir, south of Iran. Journal of Applied Geophysics, 2014, 109: 80-87.

Iglauer, S., Al-Yaseri, A. Z., Wolff-Boenisch, D. Basalt-CO_2-brine wettability at storage conditions in basaltic formations. International Journal of Greenhouse Gas Control, 2020, 102: 103148.

Iglauer, S., Pentland, C., Busch, A. CO_2 wettability of seal and reservoir rocks and the implications for carbon geo-sequestration. Water Resources Research, 2015, 51(1): 729-774.

Isfehani, Z. D., Sheidaie, A., Hosseini, M., et al. Interfacial tensions of (brine+H_2+CO_2) systems at gas geo-storage conditions. Journal of Molecular Liquids, 2023, 374: 121279.

Kestin, J., Khalifa, H. E., Correia, R. J. Tables of the dynamic and kinematic viscosity of aqueous nacl solutions in the temperature range 20-150 °C and the pressure range 0.1-35 MPa. Journal of Physical and Chemical Reference Data, 1981, 10(1): 71-88.

Lackner, K. S. A guide to CO_2 sequestration. Science, 2003, 300(5626): 1677-1678.

Li, X., Boek, E., Maitland, G. C., et al. Interfacial tension of (brines + CO_2):(0.864 NaCl + 0.136 KCl) at temperatures between (298 and 448) K, pressures between (2 and 50) MPa, and total molalities of (1 to 5) mol·kg^{-1}. Journal of Chemical & Engineering Data, 2012, 57(4): 1078-1088.

Lucas, R. Rate of capillary ascension of liquids. Kolloid Zeitschrift, 1918, 23(15): 15-22.

Mason, G., Morrow, N. R. Developments in spontaneous imbibition and possibilities for future work. Journal of Petroleum Science and Engineering, 2013, 110: 268-293.

Metz, B., Davidson, O., De Coninck, H., et al. Ipcc Special Report on Carbon Dioxide Capture and Storage. Cambridge, United Kingdom, Cambridge University Press, 2005.

Michaelides, E. E. A new model for the lifetime of fossil fuel resources. Natural Resources Research, 2017, 26(2): 161-175.

Muhammed, N. S., Haq, B., Al Shehri, D., et al. A review on underground hydrogen storage: Insight into geological sites, influencing factors and future outlook. Energy Reports, 2022, 8: 461-499.

Neuman, S. P. Theoretical derivation of darcy's law. Acta

Mechanica, 1977, 25(3): 153-170.

Niu, B., Al-Menhali, A., Krevor, S. C. The impact of reservoir conditions on the residual trapping of carbon dioxide in berea sandstone. Water Resources Research, 2015, 51(4): 2009-2029.

Palmer, G. Renewables rise above fossil fuels. Nature Energy, 2019, 4(7): 538-539.

Pan, B., Clarkson, C. R., Atwa, M., et al. Spontaneous imbibition dynamics of liquids in partially-wet nanoporous media: Experiment and theory. Transport in Porous Media, 2021, 137(3): 555-574.

Pan, B., Yin, X., Zhu, W., et al. Theoretical study of brine secondary imbibition in sandstone reservoirs: Implications for H_2, CH_4, and CO_2 geo-storage. International Journal of Hydrogen Energy, 2022, 47(41): 18058-18066.

Pentland, C. H., El-Maghraby, R., Iglauer, S., et al. Measurements of the capillary trapping of super-critical carbon dioxide in berea sandstone. Geophysical Research Letters, 2011, 38(6): L06401.

Pfeiffer, W. T., Bauer, S. Subsurface porous media hydrogen storage-scenario development and simulation. Energy Procedia, 2015, 76: 565-572.

Plug, W. J., Slob, E., Bruining, J., et al. Simultaneous measurement of hysteresis in capillary pressure and electric permittivity for multiphase flow through porous media. Geophysics, 2007, 72(3): A41-A45.

Qin, C., Wang, X., Hefny, M., et al. Wetting dynamics of spontaneous imbibition in porous media: From pore scale to darcy scale. Geophysical Research Letters, 2022, 49(4): e2021GL097269.

Selley, R. C., Cocks, L. R. M., Plimer, I. R. Encyclopedia of Geology. Amsterdam, The Kingdom of the Netherlands, Elsevier, 2005.

Tarkowski, R. Underground hydrogen storage: Characteristics and prospects. Renewable and Sustainable Energy Reviews, 2019, 105: 86-94.

Tokunaga, T. K., Wan, J., Jung, J., et al. Capillary pressure and saturation relations for supercritical CO_2 and brine in sand: High-pressure P_c (S_w) controller/meter measurements and capillary scaling predictions. Water Resources Research, 2013, 49(8): 4566-4579.

Tonnet, N., Mouronval, G., Chiquet, P., et al. Petrophysical assessment of a carbonate-rich caprock for CO_2 geological storage purposes. Energy Procedia, 2011, 4: 5422-5429.

Washburn, E. W. The dynamics of capillary flow. Physical Review, 1921, 17(3): 273-283.

Xu, T., Tian, H., Zhu, H., et al. China actively promotes CO_2 capture, utilization and storage research to achieve carbon peak and carbon neutrality. Advances in Geo-Energy Research, 2022, 6(1): 1-3.

Yang, L., Wang, S., Cai, J., et al. Main controlling factors of fracturing fluid imbibition in shale fracture network. Capillarity, 2018, 1(1): 1-10.

Zeng, L., Hosseini, M., Keshavarz, A., et al. Hydrogen wettability in carbonate reservoirs: Implication for underground hydrogen storage from geochemical perspective. International Journal of Hydrogen Energy, 2022, 47(60): 25357-25366.

Zhang, L., Chen, L., Hu, R., et al. Subsurface multiphase reactive flow in geologic CO_2 storage: Key impact factors and characterization approaches. Advances in Geo-Energy Research, 2022, 6(3): 179-180.

Zhang, L., Nowak, W., Oladyshkin, S., et al. Opportunities and challenges in CO_2 geologic utilization and storage. Advances in Geo-Energy Research, 2023, 8(3):141-145.

Zivar, D., Kumar, S., Foroozesh, J. Underground hydrogen storage: A comprehensive review. International Journal of Hydrogen Energy, 2021, 46(45): 23436-23462.